Clogging of soft particles in two-dimensional hoppers

Xia Hong, Meghan Kohne, Mia Morrell, Haoran Wang, and Eric R. Weeks
Department of Physics, Emory University, Atlanta, Georgia 30322, USA
(Received 1 November 2017; published 7 December 2017)

Using experiments and simulations, we study the flow of soft particles through quasi-two-dimensional hoppers. The first experiment uses oil-in-water emulsion droplets in a thin sample chamber. Due to surfactants coating the droplets, they easily slide past each other, approximating soft frictionless disks. For these droplets, clogging at the hopper exit requires a narrow hopper opening only slightly larger than the droplet diameter. The second experiment uses soft hydrogel particles in a thin sample chamber, where we vary gravity by changing the tilt angle of the chamber. For reduced gravity, clogging becomes easier and can occur for larger hopper openings. Our simulations mimic the emulsion experiments and demonstrate that softness is a key factor controlling clogging: with stiffer particles or a weaker gravitational force, clogging is easier. The fractional amount a single particle is deformed under its own weight is a useful parameter measuring particle softness. Data from the simulation and hydrogel experiments collapse when compared using this parameter. Our results suggest that prior studies using hard particles were in a limit where the role of softness is negligible, which causes clogging to occur with significantly larger openings.

DOI: 10.1103/PhysRevE.96.062605

I. INTRODUCTION

Flowing sand differs qualitatively from flowing fluid and understanding the differences leads to interesting physics [1,2]. A dramatic difference is seen in the gravity-driven flow of sand out of a hopper: when the exit opening from a hopper is small, the sand can clog at the hopper exit [3,4]. The existence of a critical exit opening size of 3–6 particle diameters has been long known [5–11]. Even when the hopper opening is slightly larger, and clogs do not form, the flow is influenced by the possibility of clogging: for example, there are fluctuations of the flow rate of the sand [3,12–14]. The mean flow rate is a function of the difference of the opening size to the critical size for clogging, a result often attributed to Beverloo [7] although mentioned by earlier authors as well [5]; the history is discussed in Ref. [8]. In this sense, understanding what happens when hoppers clog—and the size of the opening that causes clogging—is crucial for understanding the flow properties when the opening is larger than the critical size [4,7,8]. We note that some experiments suggest that clogging does not have a critical size but rather becomes exponentially unlikely as the hopper opening increases [15–17]; nonetheless, it's clear that understanding the flow properties requires understanding the clogging probability.

The clogging process itself is due to arch formation at the hopper exit [13,16,18,19]. The difficulty of forming large arches is the reason why hoppers do not clog when their exit opening is sufficiently large [18]. Friction may be important for the formation of these arches [18], and more generally it has long been seen that friction influences hopper flow to an extent [5,8,12,14,20]. However, it was unclear exactly how friction played a role—friction influences the angle of repose [20] and the packing density [7], for example, but it was unclear which of these (if either) influences the flow rate or clogging. Another experiment studied the shapes of arches formed in two-dimensional (2D) granular hoppers, finding that these shapes differed somewhat from simulated frictionless arches [21]; static friction allowed some arches to form that would be unstable in a frictionless situation.

The role of particle softness has been less studied. One experiment studied the flow of foams and showed that the softness of the bubbles influenced the flow [22]. In this case, there was no static friction. Due to the ability of bubbles to deform, clogging required the exit orifice to be smaller than the mean bubble size, and this profoundly changed the flow rate at larger exit orifice sizes [22] as compared to the granular Beverloo flow law [7]. One recent experiment used repulsive magnetic particles in a quasi-2D hopper and reported clogging for small orifices but did not systematically study clogging [23]. In that work, the particles repelled each other at moderate separations, and so it was not clear how the clogging related to the particle size (or even how to define that size). A pair of papers simulated the flow of softer frictional particles through 2D hoppers, and they found that as the driving force increased by a factor of 10^4 there was a mild decrease in clogging [24,25]. A key result was that as the driving force was decreased toward zero, there was a clear finite probability for clogging, suggesting that geometric effects are important [25].

In this paper we study clogging in flow out of a hopper using two quasi-two-dimensional experiments with soft nearly frictionless granular materials, and also simulations of soft frictionless particles. Our first experiment is an emulsion composed of oil droplets in water, stabilized by a surfactant, as shown in Figs. 1(a) and 1(b). The droplets are sandwiched between two parallel pieces of glass so that they are deformed into pancakelike disks [26]. In our experiments droplets only clog when the hopper opening is less than two diameters wide. Clogging arches involve only one or two droplets. Our second experiment uses soft hydrogel particles in a thin sample chamber as shown in Fig. 1(c). The influence of gravity is varied by changing the tilt angle of the chamber. Reducing the influence of gravity enhances clogging, allowing clogs to occur for hopper openings ranging from 1.5 to 2.5 diameters wide. Our results are a strong contrast to prior experimental results, which used hard frictional granular particles, which saw larger arches, and which clogged at larger opening sizes [6,14,16,18,27]. To vary the particle softness,

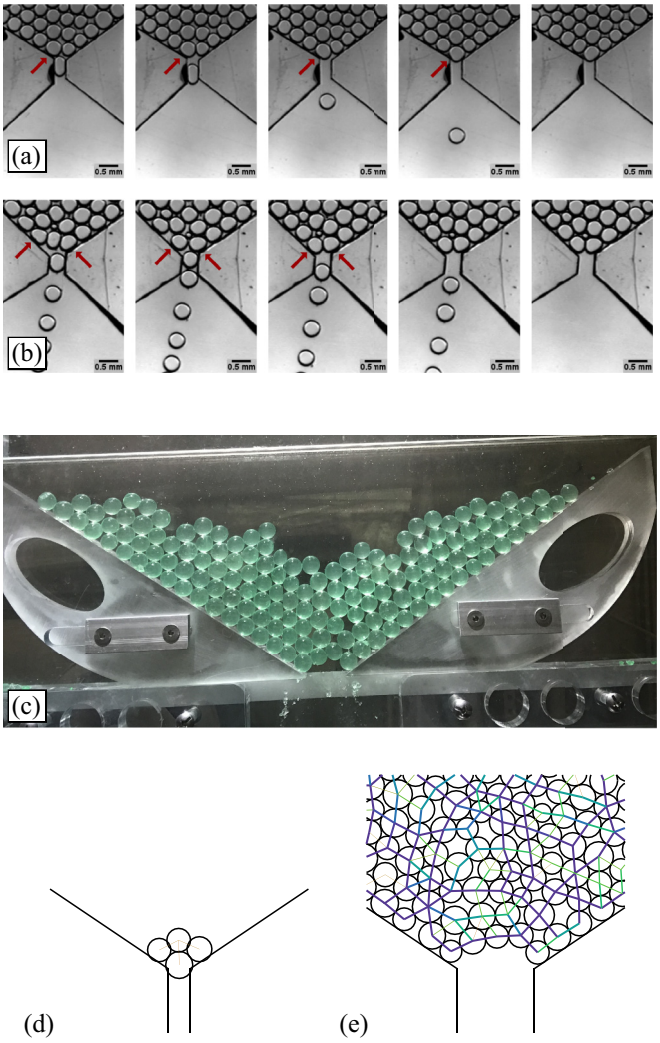

FIG. 1. (a) Clogging of oil droplets in water passing through a hopper with exit width $w/d = 0.81$ with mean droplet diameter $d = 370$ μm. The images are each 10 s apart, except for the final image, which is 50 s later. (b) Clogging with an arch composed of two oil droplets with $w/d = 1.00$ where $d = 410$ μm. The images are each 5 s apart, except for the final image, which is 30 s later. In (a) and (b) the arrows indicate the droplet(s) that will clog the opening. (c) Photograph of the hydrogel experiment in a clogged state. The sample chamber is tilted at an angle $\theta = 10^\circ$ from the horizontal and the opening width is $w = 28.8$ mm $= 2.2d$ in terms of the mean particle diameter $d = 1.31$ mm. (d, e) Simulated clogging arches. The parameter values are (d) $g/F_0 = 10^{-1}$, $w/d = 0.87$, 4 droplets left in hopper; (e) $g/F_0 = 10^{-4}$, $w/d = 3.0$, 708 droplets left in hopper. The colored lines indicate contact forces between the droplets, relative to the gravitational force acting on an isolated droplet of the mean size. The thickest (purple) lines correspond to forces 8 or more times larger than the reference force.

we conduct simulations using the Durian bubble model [28] with the particles a few orders of magnitude softer than previously studied [24,25]. The simulation results show that the softness of the experimental particles explains the difficulty of clogging; Fig. 1(d) shows a situation where the particles are quite soft, and Fig. 1(e) where they are harder. Our simulation results suggest that making the particles harder (or reducing gravity) can potentially recover the previous experimental results for hard particles. This demonstrates the importance of softness to the clogging process and shows that flowing particulate materials behave qualitatively different when the particles are easily deformable by the flow.

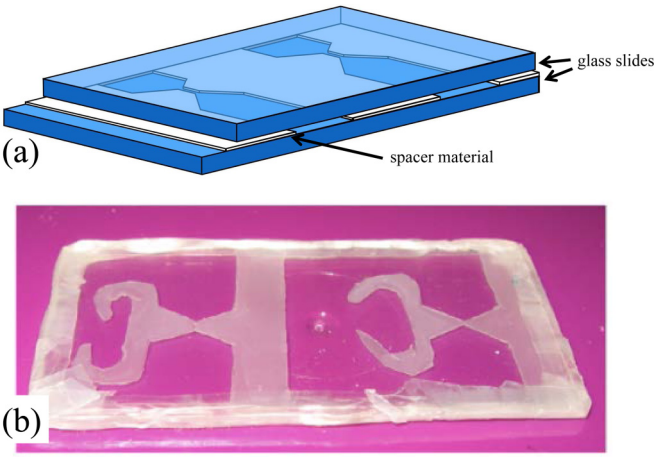

FIG. 2. (a) Sketch of a sample chamber for our emulsion experiments. (b) Photograph of a typical sample chamber constructed from parafilm. This slide contains two separate hopper chambers that are not interconnected.

II. METHODS

A. Emulsion experiment

Our samples are oil-in-water emulsions prepared by a standard coflow microfluidic technique [29]. In this technique, mineral oil (Fisher Scientific O121-1, density $\rho_{\text{oil}} = 0.83$ g/ml) is injected into a flowing stream of distilled water and surfactant. We use Fairy dishwashing detergent at mass fraction 0.025 as the surfactant, as has been done in previous work [26]. The microfluidic technique produces droplets of a desired size with 3% polydispersity. We control the size of the droplets by varying the flow rates of the oil and water in the microfluidic device. Typically we make droplets $\sim$200 μm in diameter. In some cases we mix together two batches of droplets with different sizes, but for most of our results we study samples composed of a single batch of droplets. Sometimes the emulsion gets sheared when we add it to the sample chamber, resulting in a few droplets that are unusually small, or the coalescence of droplets so that some are unusually large. Examples of each can be seen in Fig. 3.

Each sample chamber is a sandwich of a spacer between two glass slides, as shown in Fig. 2(a). The spacer material is either transparent plastic film ($\approx$120 μm thickness) or parafilm ($\approx$130 μm thickness). For each of these, the spacer material is cut into a desired shape using scissors. We briefly put the parafilm chambers onto a hot plate to slightly melt the parafilm to seal the chamber. In each case, after the initial preparation, the sample chambers are additionally sealed with epoxy to prevent leakage or evaporation. As we use scissors and position the spacer materials onto the slides by hand, often the sample chambers are imperfect. However, given the simplicity and rapidity of making these chambers, we simply select the best

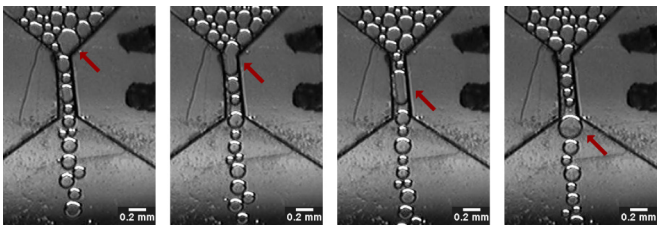

FIG. 3. This image sequence shows how a big droplet (marked with the arrow) can deform and squeeze through the hopper exit, if the surface tension is too low. The images are shown at 10-s time intervals.

sample chambers to use in our experiments, where the hopper exit is adequately shaped. Examples are shown in Figs. 1(a), 1(b) and 3. The hopper angles are set to be 32–35°, close to To *et al.*'s experiment with an angle of 34° [18].

Should droplets flowing through the hopper clog, we need a way to unclog the system and get all of the droplets back to the entrance side of the hopper. We design our sample chambers with a side channel as shown in Fig. 2(b). This allows the sample chamber to be tilted and gives a path to move droplets from one side of the hopper to the other. The "C" shape on the left side of the individual chambers shown in Fig. 2(b) is to collect and hold any air bubble that might be present after the emulsion is added to the chamber.

Given the fairly large size of the droplets, we use a CCD camera and a macrozoom lens to view our experiments, back-lighting the sample chamber. Jammed hoppers can also be seen by eye, which makes it possible to collect statistics without the camera. Video microscopy is used to count the number of droplets within a sample chamber, and to get an accurate measurement of the hopper angle of each chamber.

B. Physics of flowing emulsions

While we are motivated by experiments on granular hopper flows, as described in Sec. I, there are several differences in our emulsion experiment. These differences are described in this section.

A superficial difference is that the density of the mineral oil droplets is smaller than water, so our droplets float upward due to gravity. To make easier conceptual comparison with granular hoppers, we rotate all of our photographs so that the droplets are moving downward, for example, Figs. 1(a) and 1(b).

A second difference is that our droplets are soft and deformable. The original work by To *et al.* used steel disks [15,18,19,30], some authors use solid spheres [3,16,17,21], and others use slightly deformable photoelastic disks [14,27]. Our droplets are significantly more deformable. In the absence of external forces, a droplet would be spherical due to surface tension. However, in our experiment, droplets could potentially decrease their gravitational potential energy by deforming to squeeze through the hopper. This is indeed what happens if the surface tension is too small, or if the droplets are too large: an example is seen in Fig. 3. As the gravitational energy over a length scale d scales with droplet diameter as d^4 while surface energy scales as d^2, larger droplets will prefer to deform to reduce their gravitational energy [31]. Accordingly, to study clogging in our hoppers, we use a low amount of surfactant to keep the surface tension high, and also we use smaller droplets. This prevents the problem seen in Fig. 3. Were we to use large droplets, they would still clog if the hopper opening was sufficiently narrow, but this would then be entirely a surface tension effect rather than a study of clogging.

A third difference between our experiments and the prior granular experiments is that our oil droplets move through a viscous background fluid (water, viscosity $\eta \approx 1$ mPa s). The mineral oil droplets are themselves viscous ($\eta \approx 20$ mPa s) and experience viscous drag with the glass slides. The droplets contact the glass slides with a contact angle of 19° [26]; in other words, there is no lubricating water layer between the droplets and glass. The viscous drag on the droplets means that they move slowly with a free fall velocity of $U = 0.20$–0.25 droplet diameters per s depending on the conditions. This is in contrast to the granular experiments where particles spill out of the hopper quite rapidly [27]. This in principal might make clogging easier, as droplets moving toward the hopper exit have less inertia. The Reynolds number $\mathrm{Re} = \rho \eta_{\mathrm{water}} U/d$ is about 0.25, indicating inertia is relatively unimportant even for the fastest moving droplets. Of course, prior 2D granular experiments have some viscous drag from air, and also experience some sliding friction against their confining walls [16,18].

A fourth difference is that in a granular container, the pressure is independent of depth (apart from near the free surface at the top, and at the bottom near the exit). This is known as the Janssen effect [32], and it is due to the frictional forces acting on the particles from the container sidewalls [8,33]. Due to our droplets not having static friction, we would not expect the Janssen effect to be present in our experiment. The lack of a Janssen effect was confirmed by an earlier experiment by our group, which found the internal pressure within a similar quasi-2D emulsion pile depended on depth in a tall container [26]. This also is similar to a granular hopper experiment using submerged particles [11], which did not find a Janssen effect. Accordingly, we might expect that clogging is less likely at the start of our experiment when the weight of the pile can more easily break an arch. On the other hand, the density mismatch between the oil and water is only $\Delta\rho = 0.17$ g/ml, so the gravitational forces acting on our droplets are small albeit necessary for driving the hopper flow.

To be clear, the Janssen effect is thought to be irrelevant for understanding hopper flow. For example, one experiment removed the influence of gravity and provided strong evidence the Janssen effect is unrelated to clogging and flow rates through hoppers [10]. It is well known that granular hopper flow is independent of the amount of material in the hopper, as long as the amount of material is above some minimal threshold [7,10,17]. In contrast, that should not be the case in our experiments (and this contrast is confirmed by our simulations). As the weight above the droplets at the exit decreases, the probability of clogging increases. In other words, our experiment cannot be treated as in steady state, in contrast to granular hoppers [4,17]. For granular experiments, the existence of a steady state allows one to focus on the amount of material flowing out between clogs, using some method of unjamming a clog [17,21]. In contrast, our experimental

protocol is based on To *et al.* where we study the probability for the hopper to completely drain for a fixed initial number of droplets [18,19].

C. Hydrogel particle methods

We use soft hydrogel particles for a second series of clogging experiments. The particles are a polyacrylamide gel (green water beads, purchased from Gift Square Décor, Amazon.com). As purchased they are dry spheres around 1 mm in diameter. We swell these in distilled water for 24 h. They are fairly polydisperse, so we sieve the swollen particles. After sieving, the mean particle diameter is 13.1 mm, with a standard deviation of 0.5 mm. We place these particles in an acrylic hopper chamber with thickness 17.0 mm so that the particles are constrained to a quasi-2D geometry, as shown in Fig. 1(c). The particles start in an upper storage chamber, which has a bottom metal plate inserted holding the particles in that chamber. We initiate the experiment by rapidly removing that plate by hand, allowing the particles to fall downward toward the hopper. An identical storage chamber is placed below the hopper to contain all particles that fall through the hopper.

The sides of the hopper are at 34° angles to match the emulsion experiments. The opening width is adjustable; prior to each experiment, the hopper blocks are pushed together against an inserted plastic block of the desired width. If the experiment clogs, we move the hopper walls apart to drain the system and then reset the walls to the correct opening width.

The entire system is mounted on a horizontal axle so that we can rotate the apparatus to any angle θ relative to the horizontal. This allows us to vary the component of gravity in the plane of the hopper by a factor of 6, from full gravity ($\theta = 90^\circ$) to reduced gravity ($\theta = 10^\circ$, thus $g = g_0 \sin 10^\circ \approx 0.17 g_0$). For $\theta < 10^\circ$ the particles can form a tall pile in the bottom storage container which interferes with those flowing out of the hopper exit.

We use a TA Instruments AR2000 rheometer with a parallel-plate geometry to measure several physical properties of our hydrogel particles. We first measure the Poisson ratio. This is done by hand-cutting individual hydrogel particles into roughly cubical shapes. We then slowly compress the cubes with the rheometer using a flat plate, and image the cubes from the side during the compression and subsequent decompression. The relation between vertical strain and horizontal strain is linear, leading to a Poisson ratio of $\nu = 0.27 \pm 0.03$ (the uncertainty is the standard deviation of four measurements). This measurement is in agreement with a theory predicting $\nu \approx 0.3$ for a polymer gel with the Flory-Huggins $\chi \approx 0.5$ [34]. It is also not far from the range of Poisson ratio values measured by a prior experiment ($\nu = 0.38$–0.49) [35].

We next find the Young's modulus of the hydrogel particles by compressing individual spherical particles with the rheometer, which measures the normal force as a function of the rheometer plate position. The resulting relation between displacement and compression force is well fit by the Hertzian force law. From the Hertzian fit and using the mean value for the Poisson ratio, the Young's modulus is $E = 140 \pm 30$ kPa (the uncertainty is the standard deviation of five measurements).

To measure the friction coefficient we attach acrylic disks to the rheometer tool and base plate and compress a pair of hydrogels placed symmetrically a distance R from the rheometer axis. The particles are each trapped in small wells made from glue to prevent rolling. The rheometer measures the torque τ required to rotate the top acrylic disk with a given normal force N. We compute the friction coefficient due to the pair of particles from $\mu = \tau/2NR$, finding $\mu = 0.006 \pm 0.004$, confirming that the hydrogel particles are nearly frictionless. This is the same order of magnitude as prior measurements [36]. The variability is likely due both to heterogeneities of the particles and also the variability of the contact, which can sometimes trap water [37]. Likely μ varies within our clogging experiment; the main point is that it is always small [36]. We did not measure the hydrogel-hydrogel friction coefficient although prior work found that it is no more than 0.03 [38].

Similar to our emulsion droplet experiments, the hydrogel particles are softer than prior granular experiments, and so the pile of particles has an internal pressure that acts like a hydrostatic pressure: the more particles in the hopper, the larger the force on the particles at the exit of the hopper. There is no noticeable Janssen effect for the depth of filling we use, as confirmed by a different experiment with similar hydrogel particles [39]. In contrast to our emulsion experiments, the hydrogel particles fall through air, so there is less viscous damping.

D. Simulations

Due to challenges in experimentally varying parameters such as surface tension or gravity over a wide range, we also simulate the hopper flow of emulsions. This is done with the Durian "bubble model" [28], using the version presented in Ref. [40] that allows each particle to have a variable number of nearest neighbors. While the model was designed for bubbles in flowing foams, it also works for emulsion droplets. The simulation is strictly two-dimensional. Each droplet feels several forces. First is a repulsive contact force acting on droplet i from each neighboring droplet j, modeled as

$$\vec{F}_{ij}^{\,\text{contact}} = F_0 \left[\frac{1}{|\vec{r}_i - \vec{r}_j|} - \frac{1}{|R_i + R_j|} \right] \vec{r}_{ij}, \tag{1}$$

using the droplet radii R_i, their positions $\vec{r}_i$, and the vector $\vec{r}_{ij} = \vec{r}_j - \vec{r}_i$. The neighbors j are defined as those droplets for which $|\vec{r}_{ij}| < R_i + R_j$. F_0 acts like a spring constant and conceptually is due to the surface tension. In this model, rather than trying to deal with the droplet surface energy directly via describing the deformed droplet surface, droplets are treated as undeformed circles, which repel each other only when they overlap. Neighboring droplets also exert viscous forces on each other if they move at different velocities,

$$\vec{F}_{ij}^{\,\text{viscous}} = b(\vec{v}_i - \vec{v}_j). \tag{2}$$

To model our emulsion experiment, we add three additional forces. First, we add in a repulsive force from the hopper walls similar to Eq. (1),

$$\vec{F}_i^{\,\text{wall}} = F_0 \left[\frac{1}{|\vec{r}_i - \vec{r}_{\text{wall}}|} - \frac{1}{R_i} \right] \hat{r}_{i,\text{wall}}, \tag{3}$$

where $\vec{r}_{\text{wall}}$ is placed at the closest point on a wall to the droplet, and $\hat{r}_{i,\text{wall}}$ is a unit vector pointing normal to the wall. Similar to the droplet-droplet contact forces, $\vec{F}_i^{\text{wall}}$ only acts if a droplet overlaps with the wall, that is, if it is within a distance R_i to the wall. Second, we add in a gravitational force proportional to the mass of each droplet,

$$\vec{F}_{ij}^{\text{gravity}} = -\rho g R_i^2 \hat{y}, \tag{4}$$

which points in the $-\hat{y}$ direction and introduces the 2D density ρ and acceleration due to gravity g. Third, we add in a viscous force between the droplets and the confining plates,

$$\vec{F}_{ij}^{\text{plates}} = -c R_i^2 \vec{v}_i, \tag{5}$$

which enforces a terminal velocity (equal to $\rho g/c$) for freely falling isolated droplets. Finally, following the original bubble model method [28,40], we note that we are modeling a regime where inertia plays no role, and therefore these forces sum to zero for each droplet i:

$$\sum_j \left[\vec{F}_{ij}^{\text{contact}} + \vec{F}_{ij}^{\text{viscous}}\right] + \vec{F}_i^{\text{wall}} + \vec{F}_i^{\text{gravity}} - \vec{F}_i^{\text{plates}} = 0. \tag{6}$$

This can be rewritten as an equation for each droplet's velocity $\vec{v}_i$ in terms of the positions and velocities of all the droplets [40].

We simplify our simulations by setting $\rho = b = c = 1$. In practice, the viscous forces in the simulations are typically quite small, as the droplets flow slowly out of the hopper, and droplets generally move in similar directions to their neighbors ($\vec{v}_i \approx \vec{v}_j$). We simulate 800 droplets with a Gaussian radius distribution with mean $\langle R \rangle = 1$ and standard deviation $\sigma_R = 0.1$. We set $F_0 = 1$ for our simulations, unless otherwise noted, and vary g. As viscous forces are so small, the key control parameter is the nondimensional ratio $\rho g \langle R \rangle^2 / F_0$, which expresses the relative importance of gravity to the contact forces between droplets. Given $c = \langle R \rangle = 1$ we will write this parameter as the ratio g/F_0.

Equation (6) is a first-order differential equation; to solve it we integrate using the standard fourth-order Runge-Kutta algorithm. There are several possible internal time scales in our model: $b\langle R \rangle/F_0$, $c\langle R \rangle^3/F_0$, $b/\rho g \langle R \rangle$, and $c\langle R \rangle/\rho g$. Given our simplification $\langle R \rangle = \rho = b = c = 1$, these are two distinct time scales $1/F_0$ and $1/g$. $1/F_0$ is the time scale for two particles to push apart, limited by viscous drag. $1/g$ is the time scale for a particle to free fall a distance $\langle R \rangle$ and in our simulations $(1/g) \gg (1/F_0) = 1$. For the Runge-Kutta algorithm we use a time step of 0.1 for all cases except for $g = 10^{-4}$ (lowest terminal velocity case) where the time step is 1.0. We verified that the results do not change for any cases when using a smaller time step. A clog is defined to have occurred in the simulation when the maximum speed of all droplets is below $10^{-10}\rho g/c$. A time course of the velocities seen in one simulation is shown in Fig. 4, showing that once the hopper clogs, the velocities decay toward zero, and justifying our choice of $10^{-10}\rho g/c$ as a reasonable threshold for concluding that the simulation has clogged.

The velocities change very slowly, so rather than solving Eq. (6) for all velocities simultaneously, we use the previous timestep's velocity values in Eq. (2) for the neighbor velocities. Again, in practice, $\vec{F}_i^{\text{viscous}}$ is small compared to the other forces, so this is a reasonable simplification. For the simulations, the hopper angle is $\theta = 34^\circ$, and we use 800 droplets.

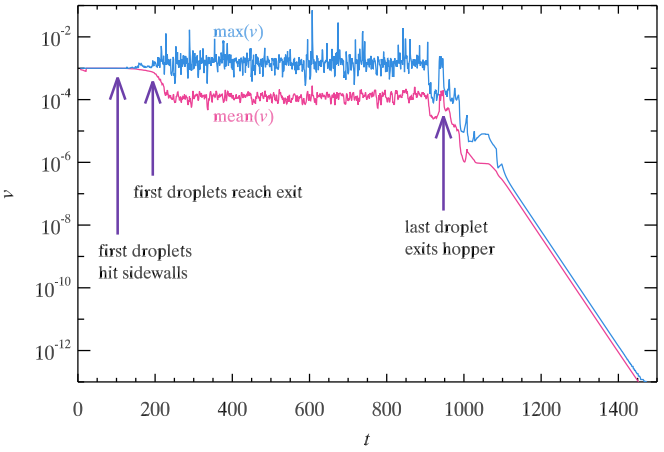

FIG. 4. The maximum velocity (blue) and mean velocity (red) as a function of time for a simulation run that clogs. The maximum and mean are taken over all droplets still in the hopper. Until the droplets first encounter the sidewalls of the hopper (first arrow), they are in free fall. Velocity fluctuations increase once the droplets are flowing through the exit (second arrow), and the velocity then decays to zero after the clog is formed (third arrow). For this simulation, the free fall velocity is given by $g = 10^{-3}$, and thus we end the simulation when the maximum velocity is below 10^{-13}. This run corresponds to a final state with a 4 droplet arch and 434 droplets left in the hopper.

We initialize the simulations by placing droplets in random positions above the hopper and with zero velocity. Initially we set the gravity in the opposite direction (away from the hopper exit). The droplets then move until they have reached positions that minimize contact forces. At that point, gravity is reversed so that the droplets fall toward the hopper exit, much like the way the emulsion experiments are conducted. The resulting pile of droplets above the hopper exit resembles the experimental conditions for both emulsion and hydrogel experiments.

III. RESULTS

A. Emulsion experiment

To determine clogging probabilities, we load our sample chamber with 750–950 droplets. We then let these droplets flow through the sample chamber and observe if a clog forms. We repeat this 50 times for each sample chamber to measure the clogging probability P_{clog} (the fraction of experiments that clog). Figure 5(a) shows P_{clog} as a function of the hopper exit width w (normalized by the mean droplet diameter d). The most striking result is that the widths at which clogging occurs are quite small. At $w/d = 1.37$, the droplets clog in half of the experiments, and for larger openings, clogging is never observed. This is in stark contrast to the case of hard frictional particles, which clog half of the time at $w/d \approx 4$ [18].

Note a caveat: the more droplets that flow through, the more chance there is to observe clogging, if the probability of clogging per droplet is nonzero [15,16,27,41]. We cannot perfectly control the number of droplets in our sample

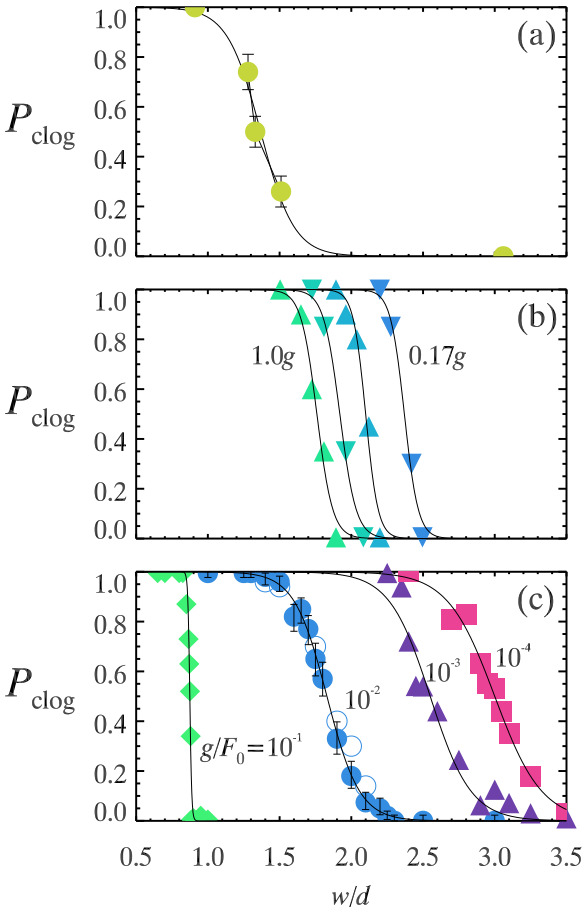

FIG. 5. The probability of clogging as a function of w/d, the ratio of the hopper exit width w to the droplet diameter d. (a) P_{clog} for the emulsion experiments (data corresponding to Table I). The solid line is a fit to the sigmoidal function $P = \{1 + \exp[(w/d - a)/b]\}^{-1}$ with $P = 1/2$ at $w/d = a = 1.37$ and width $b = 0.17$. The error bars are the uncertainty due to the finite number of trials ($n = 50$) for a Poisson process. (b) Data from the hydrogel experiments with the influence of gravity varied by setting the tilt angle at $\theta = 90°,43°,20°,10°$ from left to right. The lines are sigmoidal fits with centers $a = 1.76,1.92,2.10,2.37$ and widths $b = 0.055,0.057,0.043,0.048$ (from left to right). (c) Simulation data, with g/F_0 decreasing from left to right as labeled. For these data, $F_0 = 1$, with the exception of the open symbols for which $F_0 = 10$ (and keeping $g/F_0 = 10^{-2}$ as indicated). Typical error bars are shown for some of the data, based on the finite number of trials ($n = 100$ for the simulations). The lines are sigmoidal fits with centers $a = 0.87,1.83,2.55,3.00$ and widths $b = 0.0067,0.11,0.14,0.16$ (from left to right).

chamber, so the cases with more droplets will have P_{clog} larger. For the three points with $0 < P_{clog} < 1$, the number of droplets is fairly similar (see Table I). In the first experiment reported by To *et al.* they used 200 particles [18], approximately a quarter of the number we use. Their later work showed that with more particles P_{clog} moves to larger w/d [19]. They found $P_{clog} = 1/2$ at $w/d \approx 4.0$ for 200 particles, and ≈4.8 for 700 particles. Janda *et al.* found qualitatively similar results in their 2D granular experiment, with $P_{clog} = 1/2$ increasing from $w/d \approx 3$ with 50 particles to $w/d \approx 5.5$ with 50 000 particles [16].

TABLE I. Details of the six emulsion experiments that measured clogging probabilities. w is the hopper exit width, d the mean droplet diameter, N is the number of droplets, θ is the hopper angle, and P_{clog} is the probability of clogging based on 50 trials. The uncertainty of d is ±5 μm, and the uncertainty of w/d is ±0.03.

w/d	d	N	θ	P_{clog}
0.30	237 μm	867	32°	1.00
0.91	202 μm	947	35°	1.00
1.28	250 μm	771	33°	0.74
1.33	280 μm	786	35°	0.50
1.51	285 μm	764	33°	0.26
3.06	280 μm	923	34°	0.00

We fit our data to a sigmoidal function as shown in Fig. 5(a). This finds a width ≈0.2, slightly smaller than the widths ≈0.3 in Ref. [18]. It is not clear that the sigmoidal fit we use is correct; To *et al.* used a different fit, and their data with gear-shaped particles had a decidedly nonsigmoidal shoulder [18]. Likewise, Janda *et al.* used a different fit [16]. Our data are not sufficient to distinguish subtle differences in these fits, so we stick with the simple sigmoidal fit.

Figures 1(a) and 1(b) show two examples of clogged samples. Figure 1(a) shows $w/d \approx 0.8$ and a situation where the influence of surface tension is weak enough that one droplet can deform and slip through. However, after that first droplet, the remainder clog. Figure 1(b) shows a small "arch" of two particles that clog at $w/d \approx 1.0$.

B. Hydrogel experiments

The hydrogel experiments are done in a similar fashion to the emulsion experiments. We load the hopper with 200 particles and then allow them to flow through the hopper. We repeat this 20 times and compute P_{clog} from the fraction of times that we observe clogging. We do this for a variety of hopper opening widths w and also tilt angles θ ($\theta = 10°$, 20°,43°,90°). The results are shown in Fig. 5(b). As with the emulsions, increasing the hopper opening width decreases P_{clog} for a fixed gravitational force. However, clogging is easier than for the emulsion droplets. We observe most clogs are due to arches with three particles; at the lowest hopper openings, occasionally arches are formed with only two particles, more similar to the emulsion case. For the largest hopper openings ($w/d \approx 2.4$), occasionally arches form with four particles; an example is shown in Fig. 1(c).

The benefit of the hydrogel experiments is that the influence of gravity is apparent: clogging is easier for reduced gravity, as signified by the curves shifting to the right. The location where $P_{clog} = 1/2$ changes from $w/d = 1.76$ to 2.37 as gravity decreases by a factor of 6. For smaller gravitational forces, particles are moving slower when they first encounter the hopper walls, although in all experiments particles quickly slow down as they fill up the hopper and begin draining through the exit opening. When an arch is formed and the hopper clogs, we notice that the particles in the arch are clearly more deformed when gravity is large and/or when more particles remain in the hopper trapped above the arch. The deformation, along with the increasing P_{clog} with decreasing

gravity, suggests that particle softness plays an important role in the clogging process.

C. Simulation

We find that in our two experimental systems of soft nearly frictionless particles, the probability of clogging in hopper flow is greatly reduced from prior published experiments that studied hard frictional particles [16,18,19]. In our experiment, we only see clogging with exit apertures significantly smaller than previously seen with frictional particles [5–9,11].

The simulations allow us to vary the relative importance of gravity and contact forces over a larger range than the experiments. This is done through the ratio g/F_0 (which is nondimensional; see Sec. II D). As with the experiments, for each simulation we initialize the droplets in random positions above the hopper, let them fall, and observe if they completely flow out of the hopper or if they clog. We do $n = 100$ runs for each condition to measure P_{clog}, the fraction of runs that clog.

For a moderate value $g/F_0 = 10^{-2}$, the simulation clogging probability curve looks qualitatively similar to the experiments [circles in Fig. 5(c)]. Varying g/F_0 significantly shifts the clogging probability curve in Fig. 5(c), from $g/F_0 = 10^{-1}$ (diamonds) to $g/F_0 = 10^{-4}$ (squares). This confirms the significant role deformability plays in the clogging process, here for data where friction is not present.

Figures 1(d) and 1(e) shows examples of arches found in the simulations. For the largest value of gravity, clogging is most typically due to one large droplet that reaches the exit when most other droplets have already exited [Fig. 1(d)]. This is analogous to a droplet such as the large one shown in Fig. 3, but with fewer droplets above it such that the driving pressure is not large enough to cause the large droplet to deform. Thus, the clogging probability curve for such a large value of g/F_0 [green diamonds in Fig. 5(c)] has little to do with arch formation and more to do with the likelihood of an unusually large droplet being one of the last ones left in the hopper. Figure 1(e) shows the more interesting case for a lower value of g/F_0 corresponding to weaker gravity (or equivalently, stiffer droplets). Large arches can form (up to 5 droplets) without requiring friction to be present. This is perhaps an unsurprising result, as the theory of To *et al.* that explains their data does not require friction [18].

IV. DISCUSSION

We can compare the experimental hydrogel data and the simulation data. From the data shown in Figs. 5(b) and 5(c), we extract the hopper opening width w/d for which $P_{\text{clog}} = 0.5$. To match experiment and simulation we consider the magnitude of deformation δ/d a particle has due to its own weight (nondimensionalized by particle diameter d). We compute this for hydrogel particles by balancing the weight of one particle with the Hertz contact force law:

$$\frac{1}{6}\pi d^3 \rho g = \frac{4}{3}E^*\left(\frac{d}{2}\right)^{1/2}\delta^{3/2}, \tag{7}$$

using the particle diameter $d = 13.1$ mm, density $\rho \approx 1$ g/cm^3, $g = 9.8$ m/s^2, and $E^* = E/(1-\nu^2)$ in terms of the Young's modulus and Poisson ratio (Sec. II C). Solving this

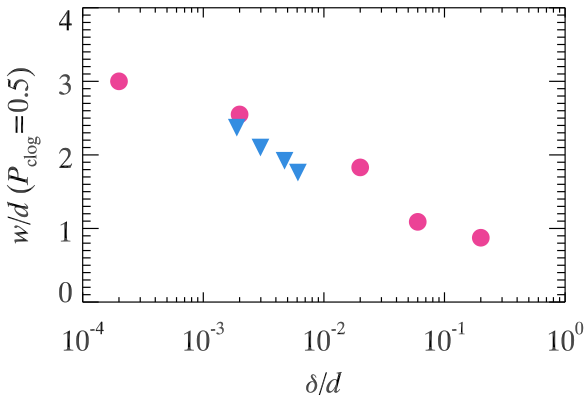

FIG. 6. A plot of the size of the hopper opening w/d for which $P_{\text{clog}} = 1/2$ as a function of δ/d, the fractional deformation of a particle due to its own weight. (This is equal to $2g/F_0$ for the simulation data; see text for discussion.) The circles are simulation data and the triangles are from the hydrogel data. The left side of the graph corresponds to lower gravity or stiffer particles. A prior experiment with 200 steel disks found $w/d = 3.7$ [18].

we find that δ/d ranges from 0.006 to 0.002 as gravity goes from maximal to minimal (when we tilt the chamber). In other words, a single hydrogel particle only deforms minimally due to gravity. A similar calculation applied to the bubble model through a balance of Eqs. (3) and (4) shows that in the bubble model $\delta/d = 2g/F_0$ (in the limit of small deformations). These calculations allows us to use δ/d to compare the simulation and experimental data. Figure 6 shows the data for the hydrogel experiments (triangles) and simulations (circles). These results are in excellent agreement given that there are no free parameters in the comparison. In fact, given the differences between the simulation (perfectly 2D, frictionless, viscous interactions) and the hydrogel experiment, the agreement is strong evidence that δ/d is a useful measure of the importance of softness. One neglected factor is that the simulations used $N = 800$ particles while the hydrogel experiments used $N = 200$; more particles in the hydrogel experiments likely would increase the probability of clogging [16] and thus slightly raise the hydrogel data in Fig. 6. For a situation with a driving force other than gravity, a similar parameter could be developed. Note that δ/d is the deformation of a particle due to its own weight; in a clogging arch with particles supported by the arch, the deformation will be significantly more.

We can compare the results of Fig. 6 to the experiments of To *et al.* that used steel disks [18]. For gear-shaped particles, they found a slightly larger value, $w/d = 4.0$ for $P_{\text{clog}} = 0.5$ as compared to $w/d = 3.7$ for the smooth disks (using 200 disks). Our results in Fig. 6 suggest that the relative influences of gravity and particle stiffness (for example as quantified by the ratio g/F_0 in the simulation) plays a more significant role for soft particles than the enhanced friction played in the prior experiments.

Our results can also be compared with centrifuge experiments of Dorbolo *et al.*, which found that clogging was uninfluenced by gravity [42]. The difference between these experiments and our work is likely explainable by their use of glass and steel beads. We can estimate the effective δ/d for their experiment. For glass beads, estimating their modulus as

$E = 70$ GPa, density as $\rho = 2.6$ g/cm^3, using their diameter $d = 400$ μm, and their maximum imposed gravity ($20g$), one finds at most $\delta/d \approx 10^{-6}$ for Ref. [42]. This is two decades lower δ/d than we have probed with our simulations. It is reasonable to conjecture that the experiments of Ref. [42] are still in a high particle stiffness limit where the clogging results are independent of gravity—equivalent to the low gravity limit of our softer particles, despite the enhanced gravity of their experiments. Comparing the results of Fig. 6 to the centrifuge experiments [42] suggests that $\delta/d \lesssim 10^{-5}$ may be sufficient to reach a limit of hard particles.

Our results are in qualitative agreement with soft frictional particle simulations of Arévalo and Zuriguel [24,25], who found that increasing gravity by four orders of magnitude decreased the clogging probability slightly. Their simulations used stiffer particles that we considered, with $\delta/d = 10^{-8}$–10^{-4}. They simulated the case where the hopper was kept continually full of particles and they measured the size of avalanches in between clogging events, so a direct comparison with Fig. 6 is not possible. As a rough comparison, for $\delta/d = 10^{-4}$ they found a mean avalanche size of $O(10^3)$ for an exit width $w/d = 4.0$ [25]. This is comparable to the number of droplets in our simulation (800) and so $w/d = 4.0$ seems roughly in agreement with the low δ/d limit of Fig. 6 as well as the steel particle results of To *et al.* [18]. Their data suggest that below $\delta/d = 10^{-5}$ one should see little dependence of P_{clog} on δ/d [25].

For large δ/d we find clogging is difficult to observe in our emulsion experiments [Fig. 5(a)]. There we find $P_{\text{clog}} = 1/2$ at $w/d = 1.37$. From Fig. 6 this corresponds to $\delta/d \approx 3 \times 10^{-2}$. This fractional deformation is consistent with visual observation of isolated droplets.

V. CONCLUSIONS

In our experiments, our soft particles cannot sustain long arches, and clogging requires small openings. One possible explanation is the lack of static friction in our experiment; our result of reduced clogging qualitatively matches the trend seen by To *et al.* who found a lower clogging probability for smooth-surface disks compared to gear-shaped disks [18]. However, our simulation results show that even frictionless droplets can form large arches under certain conditions [Fig. 1(e)]. The key requirement is that the gravitational force must be small in comparison to the stiffness of the droplets. To rephrase this in physical terms, for maximal clogging an emulsion droplet would need a high surface tension, a particle needs a large elastic modulus, or the driving force (e.g., gravity) must be low. For example, in our emulsion experiment, despite the reduced influence of gravity (due to buoyancy of the droplets) and their slower motion (due to viscous forces), gravity essentially breaks large arches due to a mechanism similar to what is seen in Fig. 3, albeit with subtler droplet deformations.

Our clogging results with reduced gravity are the opposite of those seen in prior work that found reducing forcing prevented clogging [3,43,44], and the reasons for this difference are important. The prior observation is termed "faster-is-slower" and was observed in simulations of pedestrians, where panic is counterproductive to exiting a room through a small door [43]. In later work that studied clogging in a variety of situations, the conclusion was that reducing the load on the arches at the exit allows vibrations or other noise to destroy the arch and thus the hopper flow can resume [3,45]. Or increasing the load, the weight of the grains above the exit applies a compatible load thus strengthening the arch and increasing the persistence of the clog. In contrast, our soft particles are deformed by this load which can strengthen the arch (at low loads) or break the arch (at high loads). More significantly, we have no source of incompatible forces that disrupt a stable arch once formed, unlike the prior work [3]. One could imagine a reversal of our soft particle results by adding vibrations to our macroscopic hydrogel experiment, or shrinking the oil droplet experiment so that Brownian motion becomes significant; both mechanical and thermal vibrations were shown to decrease clogging in the prior work [3]. To be clear, in both the prior work and in our work, increasing the driving force increases the outflow flux rate as long as the system is not clogged [24,25,39]; the key difference is the system behavior after a clogging arch is formed.

Overall, our results demonstrate that the flow of soft particles is qualitatively different from the case of hard particles. Hard particle behavior appears as a limiting case where the driving is low or the particle stiffness is high, such that particles are barely deformable during the flow. Our results potentially have implications for other situations where particles have soft long-range interactions such as magnetic particles [23], merging traffic [46], and perhaps flowing bacteria [47]. This may also explain why experiments with ants found no clogging with higher driving force [48].

ACKNOWLEDGMENTS

We thank D. Chen, K. Desmond, D. Durian, C. Roth, M. Thees, and I. Zuriguel for helpful discussions, and J. Burton, N. Cuccia, Y. Gagnon, and C. Orellana for help with the hydrogel mechanical measurements. This work was supported by the National Science Foundation (X.H. was supported by Grant No. CBET-1336401, M.M. and E.R.W. were supported by Grant No. DMR-1609763).

[1] H. M. Jaeger, S. R. Nagel, and R. P. Behringer, Granular solids, liquids, and gases, Rev. Mod. Phys. **68**, 1259 (1996).

[2] Y. Forterre and O. Pouliquen, Flows of dense granular media, Ann. Rev. Fluid Mech. **40**, 1 (2008).

[3] I. Zuriguel, D. R. Parisi, R. C. Hidalgo, C. Lozano, A. Janda, P. A. Gago, J. P. Peralta, L. M. Ferrer, L. A. Pugnaloni, E. Clément, D. Maza, I. Pagonabarraga, and A. Garcimartín, Clogging transition of many-particle systems flowing through bottlenecks, Sci. Rep. **4**, 7324 (2014).

[4] I. Zuriguel, Invited review: Clogging of granular materials in bottlenecks, Pap. Phys. **6**, 060014 (2014).

[5] W. E. Deming and A. L. Mehring, The gravitational flow of fertilizers and other comminuted solids, Ind. Eng. Chem. **21**, 661 (1929).

[6] R. L. Brown and J. C. Richards, Two- and Three-Dimensional flow of grains through apertures, Nature **182**, 600 (1958).

[7] W. A. Beverloo, H. A. Leniger, and J. van de Velde, The flow of granular solids through orifices, Chem. Eng. Sci. **15**, 260 (1961).

[8] R. M. Nedderman, U. Tuzun, S. B. Savage, and G. T. Houlsby, The flow of granular materials I: Discharge rates from hoppers, Chem. Eng. Sci. **37**, 1597 (1982).

[9] H. Sheldon and D. Durian, Granular discharge and clogging for tilted hoppers, Granular Matter **12**, 579 (2010).

[10] M. A. Aguirre, J. G. Grande, A. Calvo, L. A. Pugnaloni, and J. C. Géminard, Pressure Independence of Granular Flow through an Aperture, Phys. Rev. Lett. **104**, 238002 (2010).

[11] T. J. Wilson, C. R. Pfeifer, N. Mesyngier, and D. J. Durian, Granular discharge rate for submerged hoppers, Pap. Phys. **6**, 060009 (2014).

[12] R. T. Fowler and J. R. Glastonbury, The flow of granular solids through orifices, Chem. Eng. Sci. **10**, 150 (1959).

[13] D. C. Hong and J. A. McLennan, Molecular dynamics simulations of hard sphere granular particles, Physica A **187**, 159 (1992).

[14] F. Vivanco, S. Rica, and F. Melo, Dynamical arching in a two dimensional granular flow, Granular Matter **14**, 563 (2012).

[15] K. To, Jamming transition in two-dimensional hoppers and silos, Phys. Rev. E **71**, 060301 (2005).

[16] A. Janda, I. Zuriguel, A. Garcimartín, L. A. Pugnaloni, and D. Maza, Jamming and critical outlet size in the discharge of a two-dimensional silo, Europhys. Lett. **84**, 44002 (2008).

[17] C. C. Thomas and D. J. Durian, Fraction of Clogging Configurations Sampled by Granular Hopper Flow, Phys. Rev. Lett. **114**, 178001 (2015).

[18] K. To, P. Y. Lai, and H. K. Pak, Jamming of Granular Flow in a Two-dimensional Hopper, Phys. Rev. Lett. **86**, 71 (2001).

[19] K. To, P.-Y. Lai, and H. K. Pak, Flow and jam of granular particles in a two-dimensional hopper, Physica A **315**, 174 (2002).

[20] F. C. Franklin and L. N. Johanson, Flow of granular material through a circular orifice, Chem. Eng. Sci. **4**, 119 (1955).

[21] A. Garcimartín, I. Zuriguel, L. A. Pugnaloni, and A. Janda, Shape of jamming arches in two-dimensional deposits of granular materials, Phys. Rev. E **82**, 031306 (2010).

[22] Y. Bertho, C. Becco, and N. Vandewalle, Dense bubble flow in a silo: An unusual flow of a dispersed medium, Phys. Rev. E **73**, 056309 (2006).

[23] G. Lumay, J. Schockmel, D. Henández-Enríquez, S. Dorbolo, N. Vandewalle, and F. Pacheco-Vázquez, Flow of magnetic repelling grains in a two-dimensional silo, Pap. Phys. **7**, 070013 (2015).

[24] R. Arévalo, I. Zuriguel, D. Maza, and A. Garcimart'ın, Role of driving force on the clogging of inert particles in a bottleneck, Phys. Rev. E **89**, 042205 (2014).

[25] R. Arevalo and I. Zuriguel, Clogging of granular materials in silos: Effect of gravity and outlet size, Soft Matter **12**, 123 (2016).

[26] K. W. Desmond, P. J. Young, D. Chen, and E. R. Weeks, Experimental study of forces between quasi-two-dimensional emulsion droplets near jamming, Soft Matter **9**, 3424 (2013).

[27] J. Tang, S. Sagdiphour, and R. P. Behringer, Jamming and flow in 2D hoppers, AIP Conf. Proc. **1145**, 515 (2009).

[28] D. J. Durian, Foam Mechanics at the Bubble Scale, Phys. Rev. Lett. **75**, 4780 (1995).

[29] R. K. Shah, H. C. Shum, A. C. Rowat, D. Lee, J. J. Agresti, A. S. Utada, L.-Y. Chu, J.-W. Kim, A. Fernandez-Nieves, C. J. Martinez, and D. A. Weitz, Designer emulsions using microfluidics, Mater. Today **11**, 18 (2008).

[30] K. To and P.-Y. Lai, Jamming pattern in a two-dimensional hopper, Phys. Rev. E **66**, 011308 (2002).

[31] V. F. Weisskopf, Search for simplicity: Mountains, water waves, and leaky ceilings, Am. J. Phys. **54**, 110 (1986).

[32] H. A. Janssen, Versuche über Getreidedruck in Silozellen, Zeitschr. d. Vereines deutscher Ingenieure **39**, 1045 (1895).

[33] J. H. Shaxby, J. C. Evans, and V. Jones, On the properties of powders: The variation of pressure with depth in columns of powders, Trans. Faraday Soc. **19**, 60 (1923).

[34] N. Bouklas and R. Huang, Swelling kinetics of polymer gels: comparison of linear and nonlinear theories, Soft Matter **8**, 8194 (2012).

[35] U. Chippada, B. Yurke, and N. A. Langrana, Simultaneous determination of Young's modulus, shear modulus, and Poisson's ratio of soft hydrogels, J. Mater. Res. **25**, 545 (2011).

[36] J. P. Gong, Friction and lubrication of hydrogels-its richness and complexity, Soft Matter **2**, 544 (2006).

[37] T. Yamamoto, T. Kurokawa, J. Ahmed, G. Kamita, S. Yashima, Y. Furukawa, Y. Ota, H. Furukawa, and J. P. Gong, *In situ* observation of a hydrogel-glass interface during sliding friction, Soft Matter **10**, 5589 (2014).

[38] J. A. Dijksman, H. Zheng, and R. P. Behringer, Imaging soft sphere packings in a novel triaxial shear setup, AIP Conf. Proc. **1542**, 457 (2013).

[39] A. Ashour, T. Trittel, T. Börzsönyi, and R. Stannarius, Silo outflow of soft frictionless spheres, Phys. Rev. Fluids (to be published), arXiv:1708.06824.

[40] S. Tewari, D. Schiemann, D. J. Durian, C. M. Knobler, S. A. Langer, and A. J. Liu, Statistics of shear-induced rearrangements in a two-dimensional model foam, Phys. Rev. E **60**, 4385 (1999).

[41] P. G. Lafond, M. W. Gilmer, C. A. Koh, E. D. Sloan, D. T. Wu, and A. K. Sum, Orifice jamming of fluid-driven granular flow, Phys. Rev. E **87**, 042204 (2013).

[42] S. Dorbolo, L. Maquet, M. Brandenbourger, F. Ludewig, G. Lumay, H. Caps, N. Vandewalle, S. Rondia, M. Mélard, J. van Loon, A. Dowson, and S. Vincent-Bonnieu, Influence of the gravity on the discharge of a silo, Granular Matter **15**, 263 (2013).

[43] D. Helbing, I. Farkas, and T. Vicsek, Simulating dynamical features of escape panic, Nature **407**, 487 (2000).

[44] J. M. Pastor, A. Garcimartín, P. A. Gago, J. P. Peralta, C. Martín-Gómez, L. M. Ferrer, D. Maza, D. R. Parisi, L. A. Pugnaloni, and I. Zuriguel, Experimental proof of faster-is-slower in systems of frictional particles flowing through constrictions, Phys. Rev. E **92**, 062817 (2015).

[45] M. E. Cates, J. P. Wittmer, J. P. Bouchaud, and P. Claudin, Jamming, Force Chains, and Fragile Matter, Phys. Rev. Lett. **81**, 1841 (1998).

[46] D. Helbing, Traffic and related self-driven many-particle systems, Rev. Mod. Phys. **73**, 1067 (2001).

[47] E. Altshuler, G. Mino, C. Perez-Penichet, L. D. Rio, A. Lindner, A. Rousselet, and E. Clément, Flow-controlled densification and anomalous dispersion of *E. coli* through a constriction, Soft Matter **9**, 1864 (2013).

[48] S. Boari, R. Josens, and D. R. Parisi, Efficient egress of escaping ants stressed with temperature, PLoS ONE **8**, e81082 (2013).